ACS Catalysis

pubs.acs.org/acscatalysis

Research Article

Stereo- and Regioselective Dimerization of Alkynes to Enynes by Bimetallic Syn-Carbopalladation

Camilla Pfeffer, Nick Wannenmacher, Wolfgang Frey, and René Peters*

Cite This: *ACS Catal.* 2021, 11, 5496–5505

Read Online

ACCESS | Metrics & More | Article Recommendations | Supporting Information

ABSTRACT: Enynes are important motifs in bioactive compounds. They can be synthesized by alkyne−alkyne couplings for which a number of mechanisms have been suggested depending on catalyst type and dominant product isomers. Regarding bimetallic pathways, hydrometalations and anti-carbopalladations have been discussed to account for the formation of geminally substituted and (*Z*)-configured enynes, respectively. Here we report a bimetallic alkyne−alkyne coupling that yields (*E*)-configured enynes. An unusual type of acetylide Pd bridging was found in putative catalytic intermediates which is arguably responsible for the regio- and stereochemical reaction outcome. Mechanistic studies suggest that a double $\mu-\kappa:\eta^2$ acetylide bridging enables a bimetallic syn-carbometalation. Interestingly, depending on the reaction conditions, it is also possible to form the geminal regioisomer as major product with the same catalyst. This regiodivergent outcome is explained by bi- versus monometallic reaction pathways.

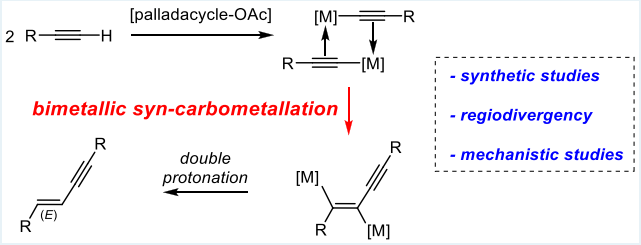

KEYWORDS: *bimetallic catalysis, carbopalladation, enynes, ferrocene, palladacycle, regioisomers*

INTRODUCTION

Conjugated enynes are established as high-value building blocks.[1] In addition, the enyne motif is present in a number of both natural and artificial biologically active compounds.[2] An atom-economic way to synthesize conjugated enynes is the dimerization of alkynes **1**.[3] A number of catalysts with, for example, iron,[4−6] ruthenium,[7] cobalt,[8,6b] rhodium,[9] iridium,[10] palladium,[3,11−15] gold,[16] yttrium,[17] and main group metal centers,[18] have been reported for this purpose. The major challenge is the control of regio- and stereoselectivity in this C,C-coupling.

In general, three different isomers can be formed in such homodimerizations of alkynes (eq 1).[3,11,12] Whereas (*E*)- and (*Z*)-configured enynes **2** are generated by "head-to-head" dimerization, the geminal regioisomer **3** is formed by "head-to-tail" dimerization.[3,11,12]

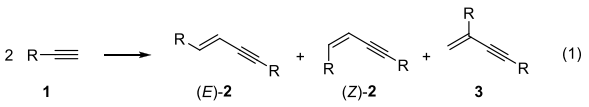

Depending on the type of catalyst, different reaction mechanisms have been suggested in order to explain the attained regio- and stereoselectivities.[11] (*E*)-**2** is often formed by hydro- or carbometalation pathways of monomeric metal acetylide acetylene complexes (Scheme 1, mechanisms 1a and 2a, respectively),[11,14,19] as both key steps proceed as syn-additions. In contrast, bimetallic acetylide/alkyne intermediates can undergo anti-additions resulting in stereoselective syntheses of (*Z*)-**2** (mechanism 4)).[20] Other mechanisms involve mono-[4,21] or bismetal[22] vinylidene intermediates resulting in (*E*)-**2** and (*Z*)-**2** (not depicted). Head-to-tail dimerization of **1** to give regioisomeric **3** was explained by monometallic syn-carbometalation[23] (mechanism 1b) and by bimetallic hydrometalation as key steps (mechanism 3).[24]

Regarding the use of Pd catalysts, monometallic Pd complexes bearing sterically demanding phosphine ligands were reported in 1987 by Trost et al. to be highly selective catalysts for the formation of the geminal products **3**.[25] A carbometalation pathway was postulated (mechanism 2b).[26]

In contrast, Nolan et al. could form (*E*)-**2** with high selectivity using a Pd−NHC complex in the presence of an excess of Cs_2CO_3 as base.[12] Gevorgyan et al. also utilized a Pd−NHC complex but in the presence of an additional electron-rich phosphine ligand to preferentially form (*E*)-**2**.[13] DFT calculations showed that this reaction is likely to proceed via hydropalladation (mechanism 1). Depending on a carboxylate additive, product **3** was also available, most likely by carbopalladation (mechanism 2b).[13] Moreover, Guo and Han reported a combination of a Pd bisphosphine complex

Received: February 2, 2021
Revised: April 12, 2021
Published: April 21, 2021

Scheme 1. Common Mechanisms for Alkyne Dimerizations and Comparison to This Work

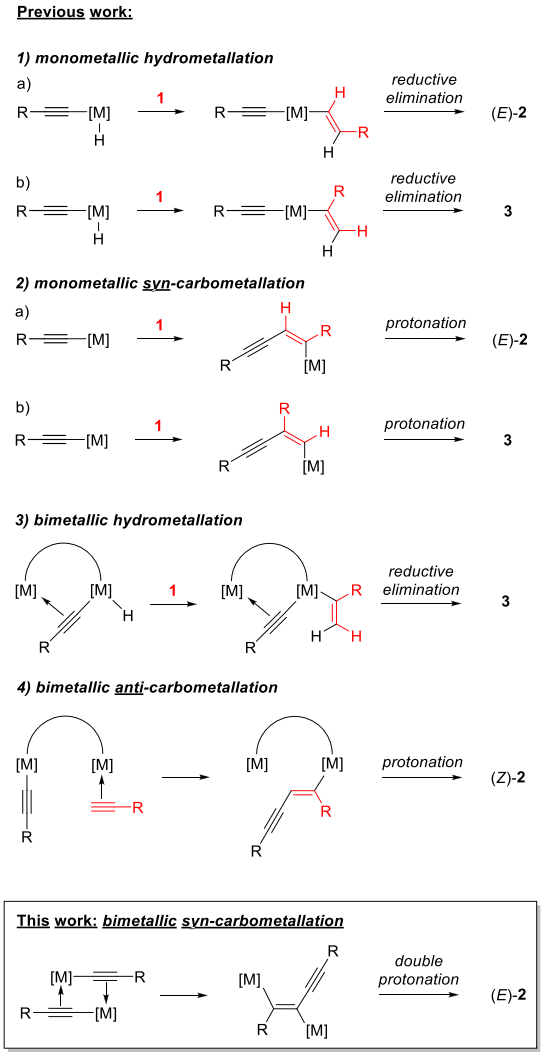

and a phosphinic acid to provide (*E*)-**2** which is believed to proceed via hydrometalation.[23]

In contrast to these studies employing neutral ligands, Shaughnessy et al. studied the use of acetate-bridged aliphatic *C*,*P*-palladacycle catalysts, which were effective in (*E*)-selective couplings of propargylic alcohols and amines.[27] Under the reported reaction conditions, an acetate/acetylide-bridged dimeric palladacycle **4** was identified (Figure 1). By X-ray analysis the acetylide ligand was found to undergo an unprecedented $\mu-\kappa^1$-coordination to both Pd(II) centers.

Herein we report a regiodivergent dimerization of alkynes **1** using a ferrocene-based *C*,*N*-palladacycle catalyst. In contrast to the above-mentioned previous studies making use of bimetallic catalysis (mechanisms 3 and 4), (*E*)-**2** was stereoselectively formed, very likely proceeding via a bispalladium complex.[28] A novel type of acetylide bridging for bis-Pd complexes[29] was found in putative catalytic intermediates. Our studies suggest that a double $\mu-\kappa:\eta^2$ acetylide bridging allows for a cooperative bimetallic syn-carbometalation, while in the above-mentioned previous bimetallic carbometalation approaches, only (*Z*)-**2** was accessible by anti-additions. Contrariwise, depending on the reaction conditions, it is also possible to form regioisomer **3** as major product with the same catalyst. This regiodivergent outcome is explained by a monometallic pathway for the formation of **3**.

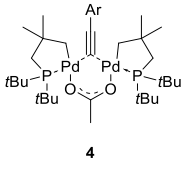

4

Figure 1. $\mu-\kappa^1$-Acetylide-bridged bis-Pd complex found in the alkyne−alkyne coupling by Shaughnessy et al.[27]

RESULTS AND DISCUSSION

Optimization of the Selective Formation of (*E*)-2. The chloride-bridged ferrocene-based palladacycle precatalysts $[FIP\text{-}Cl]_2$ (FIP = ferrocenyl imidazoline palladacycle) and $[FBIP\text{-}Cl]_2$ (FBIP = ferrocenediyl bisimidazoline bispalladacycle), which were previously developed by our group[30,31] and are accessible in high yields and in few steps, were studied as precatalysts. They were activated by different silver salts for chloride anion exchange by our previously described protocols.[30,31] The activated complexes were initially investigated in the dimerization of **1a** in chlorobenzene at 50 °C (Table 1). The best results were achieved by activation with AgOAc. Using 5.0 mol % of precatalyst, a mixture of all three isomers (*E*)-**2a**, (*Z*)-**2a**, and **3** was formed in low yields and with a moderate preference for (*E*)-**2a**. With the FIP catalyst, a higher yield (36%, entry 1) and a higher selectivity for dimerization versus tri/oligomerization was noticed (48% conversion), whereas FBIP showed higher catalytic activity (99% conversion), but the product mixture was much more complex (yield of dimer: 20%, entry 2).

A solvent screening was then performed, and with acetonitrile, a higher activity, dimerization yield, and selectivity for (*E*)-**2a** was found (entry 3). Improved selectivities were attained by slightly reducing the reaction temperature to 45 °C (entry 4) and using acetic acid (0.5 equiv) which was added to speed the protonolysis of generated Pd−vinyl bonds (entry 5). A similar result was obtained with NaOAc as additive (entry 6), probably due to generation of HOAc in the course of the catalytic cycle. Adding water (5.0 equiv) instead, this effect was not found (entry 7). Adding both NaOAc and H_2O, yield and selectivity were improved (entry 8). The product yield was further increased by additional HOAc (entry 9). Surprisingly, by reducing the precatalyst loading to 2 mol %, yield and selectivity were improved to synthetically useful values (entries 10 and 11). This is at least partly explained by no detectable alkyne trimerization as side reaction with the decreased catalyst amount. Finally a yield of 91% and an isomeric ratio (*E*)-**2a**/(*Z*)-**2a**/**3** of 94/5/1 was accomplished. No hydrogenation products were detected that might point to the formation of metal hydride intermediates.

Scope of the (*E*)-Selective Dimerization. The conditions described in Table 1/entry 11 were then used to investigate the applicability to other terminal alkyne substrates (Table 2). Using aromatic alkynes, substituents displaying different electronic effects were all accommodated. Aromatic alkynes bearing σ- (entries 3, 4, 9, 11, 12) and π-acceptors (entry 5) thus provided useful to good yields and good to excellent stereo- and regioselectivities. With an unsubstituted Ph residue, a nearly quantitative yield and high selectivities

https://doi.org/10.1021/acscatal.1c00473
ACS Catal. 2021, 11, 5496−5505

Table 1. Development of Regio- and Stereoselective Dimerization of Terminal Alkynes

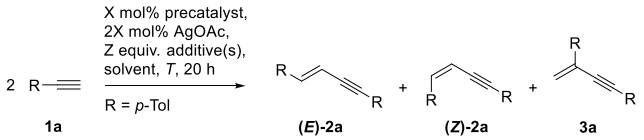

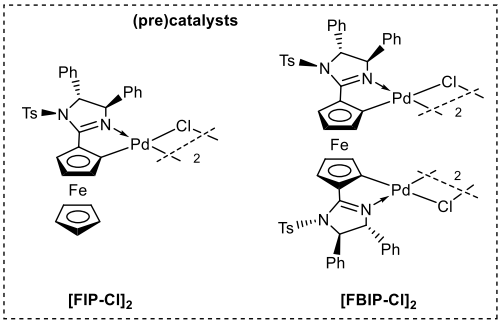

no.	$[Pd(II)Cl]_2$ (X)	additives (Z)	solvent	T (°C)	yield (%)[a]	(E)/(Z)-2a/3[b]
1	FIP (5.0)	-	PhCl	50	36	61/25/14
2	FBIP (5.0)	-	PhCl	50	20	69/16/15
3	FIP (5.0)	-	MeCN	50	64	72/7/21
4	FIP (5.0)	-	MeCN	45	60	80/9/11
5	FIP (5.0)	HOAc (0.5)	MeCN	45	60	85/7/8
6	FIP (5.0)	NaOAc (0.5)	MeCN	45	69	84/5/11
7	FIP (5.0)	H_2O (5.0)	MeCN	45	64	60/11/29
8	FIP (5.0)	NaOAc (0.5), H_2O (5.0)	MeCN	45	73	90/1/9
9	FIP (5.0)	HOAc (0.5), NaOAc (1.0), H_2O (5.0)	MeCN	45	78	86/4/10
10	FIP (2.0)	HOAc (0.5), NaOAc (1.0), H_2O (5.0)	MeCN	45	88	93/5/2
11	FIP (2.0)	HOAc (0.5), NaOAc (3.0), H_2O (5.0)	MeCN	45	91	94/5/1

[a]Yield of the mixture of (E)-**2a**, (Z)-**2a**, and **3** determined by ^{1}H NMR using mesitylene as internal standard. [b]Isomeric ratio determined by ^{1}H NMR of the crude mixture.

were obtained (entry 2). σ- (entries 1, 13) and π-donors (entries 6, 7,[32] 8, 10, 12) as well as an extended π-system (entry 14) were also well tolerated and gave rise to good to high yields and selectivities. Noteworthy is that an ortho-substituent was also well tolerated as well as conjugated enyne substrate **1n**, which formed product (E)-**2n** with exclusive stereo- and regioselectivity yet in moderate yield. Unfortunately, trimethylsilylacetylene (entry 16) as well as aliphatic alkynes (not shown) gave no dimerization product.

Regioselective Synthesis of Geminal Regioisomer 3. During the optimization of the stereo- and regioselective synthesis of (E)-**2a**, a strong solvent effect on the reaction outcome was noted. Particularly interesting was the finding that regiodivergency is enabled simply by performing the dimerization in ethyl acetate (Table 3). In the absence of additives at 50 °C a moderate preference for the formation of **3** was found (entry 1). Reducing the reaction temperature to 30 °C increased the regioselectivity yet at the expense of a low yield (entry 2). Nevertheless, in the presence of water (30 equiv) not only was the regioselectivity further improved, but also the dimerization yield was enhanced to 75% (entry 3).

The conditions of Table 3/entry 3 were applied to six different substrates (Table 4). In general, acceptor and donor substituents on the aromatic ring were tolerated in para and meta positions, albeit product yields and regioselectivity were lower than for the (E)-selective dimerization. **1p** was the most difficult substrate in terms of product yield. However, it should be mentioned that **3p** has, to our knowledge, never been prepared previously by alkyne dimerization, maybe as a result of the strong +M effect of the *N*-acetyl substituent.

Mechanistic Studies. To learn more about the title reaction, kinetic studies were performed. Blackmond's Reaction Progress Kinetic Analysis (RPKA)[33] was applied using fluorine-containing substrate **1c** in order to enable the use of ^{19}F NMR spectroscopy for monitoring (for details of the kinetic studies, see Supporting Information). In analogy to the so-called "same excess" protocol,[33] catalyst robustness and product influence were studied. The initial concentrations for the different measurements are shown in Table 5.

Figure 2 shows the corresponding reaction profiles using a decay of the concentration of **1c**. Experiment K1 (Table 5, blue curve in Figure 2) serves as standard experiment for comparison. In experiment K2 (red curves) the starting concentration of **1c** corresponds to the concentration at 50% conversion in K1.[33] A time shift shows, that this experiment proceeded faster than K1 which might suggest a partial catalyst decomposition during the first 50% of conversion in the standard experiment. In a further experiment K3 (green curves) the starting point as in K2 was used except that 50 mol % of product **2c** was added, because in the reference experiment K1 also around 50% product was present after 50% conversion. In K3 the reaction proceeded even somewhat faster than found for K2, indicating a small product acceleration. This is tentatively assigned to a catalyst stabilization by the product.

Variable Time Normalization Analysis (VTNA) developed by Burés was used to determine the empirical rate law.[34] The

https://doi.org/10.1021/acscatal.1c00473
ACS Catal. 2021, 11, 5496−5505

Table 2. Investigation of Substrate Scope and Limitations

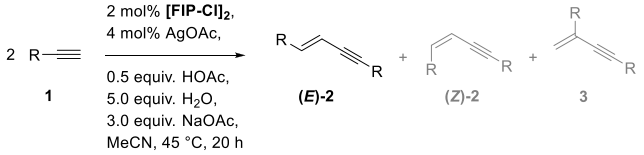

#	R	1	yield (%)[a]	(E) / (Z)-2 / 3[b]
1	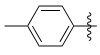	1a	91	94 / 5 / 1
2		1b	99	92 / 6 / 2
3	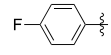	1c	71	88 / 8 / 4
4	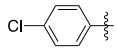	1d	65	90 / 10 / -
5	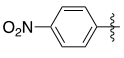	1e	63	93 / 7 / -
6	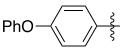	1f	77	86 / 5 / 9
7	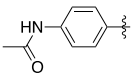	1p	>99	94 / 5 / 1
8	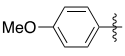	1g	94	90 / 6 / 4
9	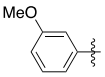	1h	74	90 / 6 / 4
10		1i	93	83 / 14 / 3
11	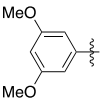	1j	79	91 / 7 / 2
12	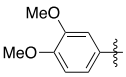	1k	69	90 / 8 / 2
13	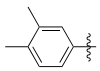	1l	90	93 / 5 / 2
14		1m	77	95 / 5 / -
15[c]		1n	37	>99 / - / -
16		1o	0	-

[a]Yield of the mixture of (*E*)-**2a**, (*Z*)-**2a**, and **3** determined by ^{1}H NMR using mesitylene as internal standard. [b]Isomeric ratio determined by ^{1}H NMR of the crude mixture. [c]5.0 mol % of [FIP-Cl]$_2$ was used.

reaction depicted in Table 5/K1 was studied in MeCN-d_3 in six experiments at 45 °C for 14 h using different initial concentrations of catalyst, substrate **1c**, acetic acid, sodium acetate, and water monitoring the concentration of **1c** by ^{19}F NMR spectroscopy (for details, see Supporting Information).

The best overlay for the normalization of the time scale axis was achieved with the following equation:

Table 3. Optimization of the Regioselective Synthesis of 3

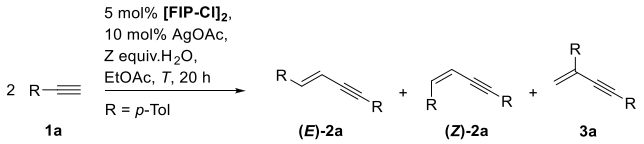

no.	Z	T (°C)	yield (%)[a]	(E)/(Z)-2a/3[b]
1	-	50	50	31/13/56
2	-	30	31	18/8/74
3[c]	30	30	75	14/5/81

[a]Yield of the mixture of (*E*)-**2a**, (*Z*)-**2a**, and **3** determined by ^{1}H NMR using mesitylene as internal standard. [b]Isomeric ratio determined by ^{1}H NMR of the crude mixture. [c]Reaction time: 48 h.

Table 4. Application of Different Substrates in the Regioselective Synthesis of 3

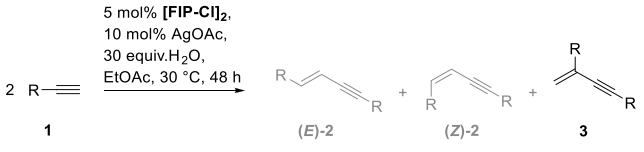

#	R	1	yield (%)[a]	(E) / (Z)-2 / 3[b]
1	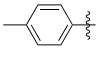	1a	75	14 / 5 / 81
2		1b	61	16 / 10 / 74
3	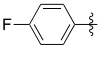	1c	52	21 / 15 / 64
4	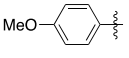	1g	65	20 / 9 / 71
5	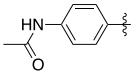	1p	57	14 / 6 / 80
6		1q	73	19 / 10 / 71

[a]Yield of the mixture of (*E*)-**2a**, (*Z*)-**2a**, and **3** determined by ^{1}H NMR using mesitylene as internal standard. [b]Isomeric ratio determined by ^{1}H NMR of the crude mixture. [c]5.0 mol % of [FIP-Cl]$_2$ was used.

Table 5. Initial Concentrations for the Reaction Progress Kinetic Analysis (RPKA)

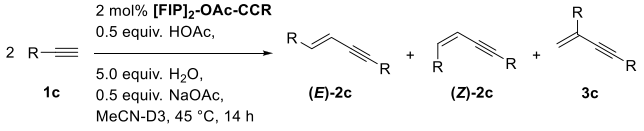

R = *p*-F-C$_6$H$_4$

experiment	[1c] (mol/L)	[FIP$_2$]-OAc-CC-*p*-F-C$_6$H$_4$ (mol/L)	[2c] (mol/L)
K1 (standard)	0.1	0.002	-
K2 (same excess)	0.05	0.002	-
K3 (product addition)	0.05	0.002	0.05

https://doi.org/10.1021/acscatal.1c00473
ACS Catal. 2021, 11, 5496−5505

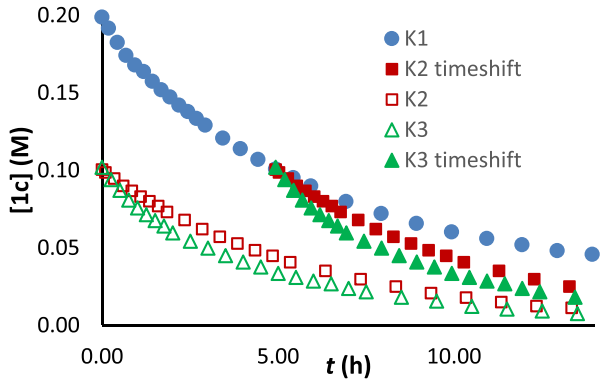

Figure 2. Reaction profiles monitoring **1c** using Blackmond's protocol[33] under the initial conditions of Table 5.

$$r = k_{obs}[\text{catalyst}]^{0.8}[\mathbf{1c}]^{2.0}[\text{HOAc}]^{0.0}[\text{NaOAc}]^{0.2}[\text{H}_2\text{O}]^{0.0}$$

The nearly first-order kinetic dependence in catalyst can be explained by a bimetallic active catalyst species formed from the bimetallic catalyst $[\text{FIP-OAc}]_2$ (generated from $[\text{FIP-Cl}]_2$ by AgOAc).[30f,h] The zero-order kinetic dependence in acetic acid and water suggests that an expected protonation step is not turnover-limiting under the developed reaction conditions. The second-order kinetic dependence in alkyne seems to suggest that the coupling event, i.e., the C−C-bond-forming step, is rate-limiting.

Based on the kinetic studies as well as spectroscopic investigations and deuteration experiments shown below, the following catalytic cycle (depicted for substrate **1a**) is proposed (Scheme 2). According to this mechanism, $[\text{FIP-OAc}]_2$ is initially transformed into the acetate/acetylide-bridged dimer $[\text{FIP}]_2$-OAc-CCR (CCR = acetylide), which could be detected by ESI mass spectrometry during the catalytic reaction (R = *p*-Tol: *m*/*z* = 1506.1067; found: 1506.1034). To receive more information about the interaction of the catalyst with a terminal alkyne, $[\text{FIP-Cl}]_2$ was treated with AgOAc (2 equiv) and a stoichiometric amount of acetylene **1e** (1 equiv). The defined complex $[\text{FIP}]_2$-OAc-CCR (R = *p*-O_2N−C_6H_4) was formed under these conditions in quantitative yield (Scheme 3).

Scheme 2. Proposed Simplified Catalytic Cycle for the Regioselective Synthesis of (*E*)-2a

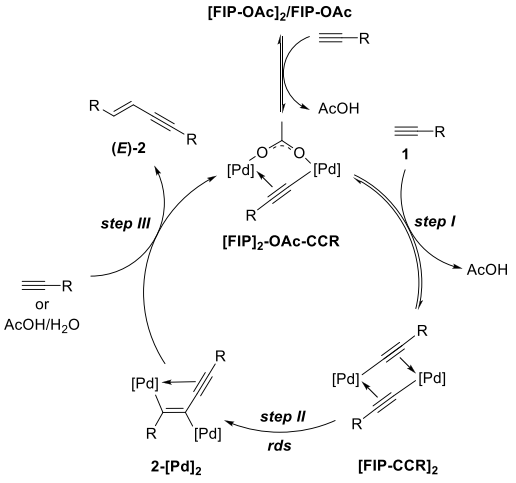

Scheme 3. Stoichiometric Formation of the Acetate/Acetylide-Bridged Dimer $[\text{FIP}]_2$-OAc-1e

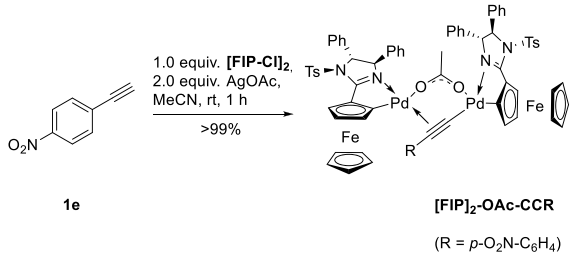

The suggested structure was confirmed by single-crystal X-ray analysis (Figure 3). Two closely related conformers were found. In these structures, the acetate ligand acts as a μ−κ^2 bridge, and the acetylide as μ−κC^{α}:η^2 bridge between both Pd(II) centers, which to our knowledge is without precedent for Pd(II) catalysts. The asymmetric bridging mode should result in an uneven charge distribution for both metal centers.[35] The acetylide bridging mode thus differs significantly from the bis-Pd−acetylide complex **4** by Shaughnessy et al.[27] shown in the Introduction.

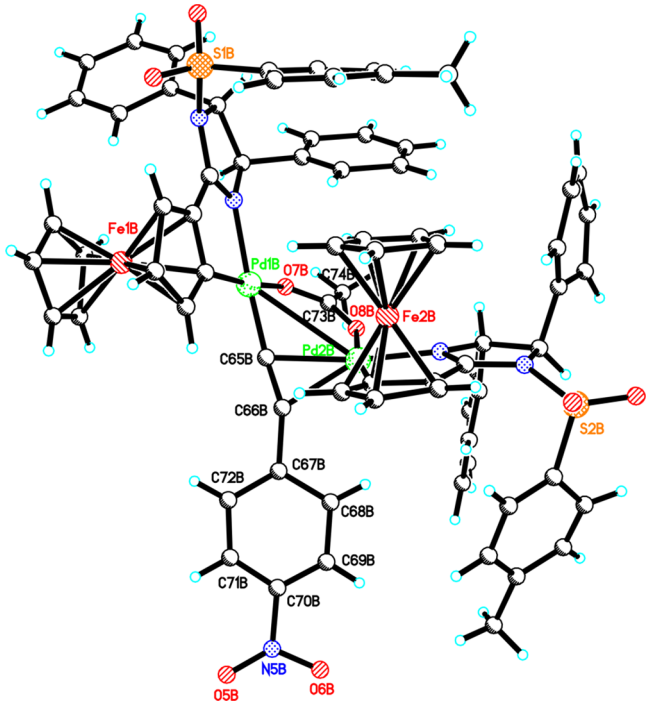

Figure 3. X-ray crystal structure analysis of the μ−κC^{α}:η^2 acetylide-bridged bis-Pd complex $[\text{FIP}]_2$-OAc-CCR (R = *p*-O_2N−C_6H_4). A visualization using thermal ellipsoids is shown in the Supporting Information.

Step I in the proposed catalytic cycle (Scheme 2) involves the subsequent formation of a C_2-symmetric bisacetylide-bridged bis-Pd(II) complex $[\text{FIP-CCR}]_2$ from $[\text{FIP}]_2$-OAc-CCR. Also in this case it was possible to form complex $[\text{FIP-CCR}]_2$ stoichiometrically (Scheme 4).

Treating $[\text{FIP-Cl}]_2$ with silver tosylate and subsequently with acetylene **1a** in the absence of acetate/HOAc provided $[\text{FIP-CCR}]_2$ (R = *p*-Tol) in 90% yield. The ^{1}H NMR spectrum of this compound shows a single set of signals. In combination

https://doi.org/10.1021/acscatal.1c00473
ACS Catal. 2021, 11, 5496−5505

Scheme 4. Stoichiometric Formation of the Bis-Acetylide-Bridged Dimer [FIP-CC*p*-Tol]$_2$

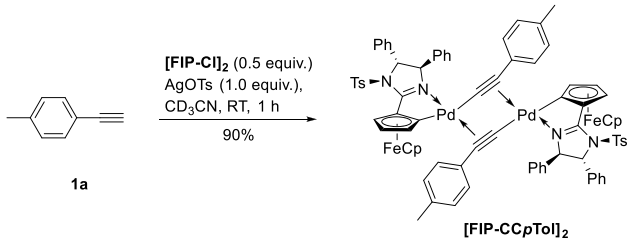

with ESI-MS results we suggest a C_2-symmetric dimeric structure with bis-μ–κC^{α}:η^2 acetylide bridging.

By ESI-MS, {[FIP]$_2$-CCR}$^+$ (R = *p*-Tol; m/z = 1445.0897; found: 1445.0893, see Supporting Information) was detected during the catalytic reaction, which might be formed by eliminating one bridging acetylide ligand from [FIP-CCR]$_2$. [FIP-CCR]$_2$ was found to be relatively stable in MeCN[36] but rapidly decomposed in chloroform and other solvents such as chlorobenzene or ethyl acetate to give free ferrocene ligand and Pd(0). Yield determination was performed by ^{1}H NMR using an internal standard.

Treating [FIP-CC*p*-Tol]$_2$ with a stoichiometric amount of **1a** in the presence of the aqueous acetate buffer resulted in a rapid equilibrium with [FIP]$_2$-OAc-CC*p*-Tol, in which the latter is dominating (ratio 1:4, Scheme 5). Within 1 min, a

Scheme 5. Rapid Equilibrium between [FIP-CC*p*-Tol]$_2$ and [FIP]$_2$-OAc-CC*p*-Tol and Slow Product Formation

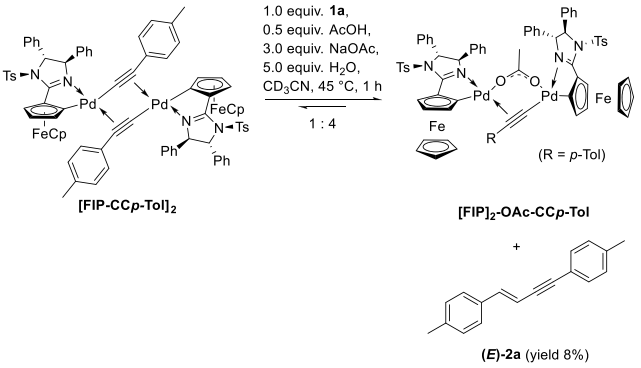

ratio of 1:3 was already noticed. After 5 min, 2% of product (*E*)-**2a** was found, after 60 min 8%. This result also suggests that C–C bond formation is slow. Moreover, during catalysis [FIP]$_2$-OAc-CC*p*-Tol was identified as major catalyst species, probably representing the catalytic resting state.

Comparison of the initial reaction rates caused by [FIP-OAc]$_2$, [FIP]$_2$-OAc-CC*p*-Tol, and [FIP-CC*p*-Tol]$_2$ showed very similar catalytic activity and productivity for all of them, suggesting that they are all catalytically relevant (for details, see Supporting Information).

In step II of the catalytic cycle (Scheme 2), an intramolecular bimetallic syn-carbopalladation step is expected, in which one acetylide acts as nucleophile attacking the side-on coordinated alkyne moiety of the other acetylide. The resulting vinyl–Pd$_2$ intermediate or more likely its precursor [FIP-CC*p*-Tol]$_2$ with the predicted isotopic pattern was detected by ESI-MS during the catalytic reaction (m/z = 1560.1445; found: 1560.1490, see Supporting Information) next to [FIP]$_2$-OAc-CC*p*-Tol.

The next step III involves the protonolysis of the Pd–C bonds. Based on the empirical rate law shown above, the detected (and isolated) catalytic intermediates [FIP]$_2$-OAc-CC*p*-Tol and FIP-CC*p*-Tol, as well as the equilibrium with slow product formation shown in Scheme 5, it is unlikely that this step is rate-limiting.

Deuteration experiments were performed employing deuterated acetylene (Scheme 6). The deuteration degree determined after a reaction time of just 3 h to minimize H/D-exchanges after product formation was found to be very low for both positions H$_A$ and H$_B$.

Scheme 6. Deuteration Experiments under (*E*)-Selective Conditions Using Deuterated Acetylene 1a-D as the Only D$^+$ Source

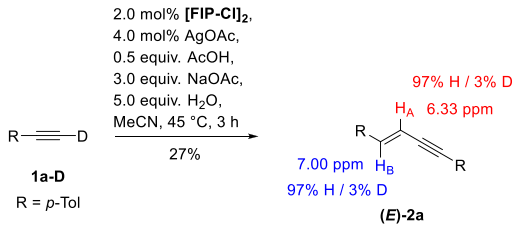

Using AcOD and D$_2$O as D$^+$ sources (Scheme 7, top), identical deuteration levels of 68% were found for H$_A$ and H$_B$.

Scheme 7. Deuteration Experiments under (*E*)-Selective Conditions Using AcOD and D$_2$O as the D$^+$ Source

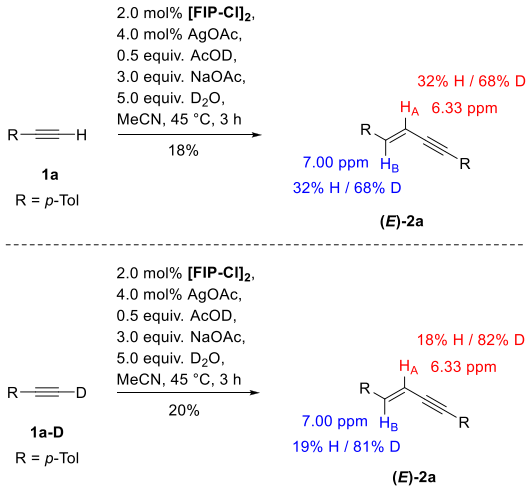

The difference from a complete deuteration level can be explained by the use of nondeuterated **1a**, which releases a proton during the Pd–acetylide formation but mainly by residual water in the NaOAc used. Using commercial "anhydrous" NaOAc gave deuteration levels of about 50%, and drying it under high vacuum increased these values to 68%. The assumption is further confirmed by the use of deuterated proton sources (DOAc, D$_2$O) in combination with deuterated acetylene **1a-D**, which provided deuteration levels of around 80% (Scheme 7, bottom).

In contrast, for the regioselective synthesis of **3** in EtOAc as solvent, we propose the mechanism depicted in Scheme 8, in

https://doi.org/10.1021/acscatal.1c00473
ACS Catal. 2021, 11, 5496–5505

Scheme 8. Proposed Simplified Catalytic Cycle for the Regioselective Synthesis of 3

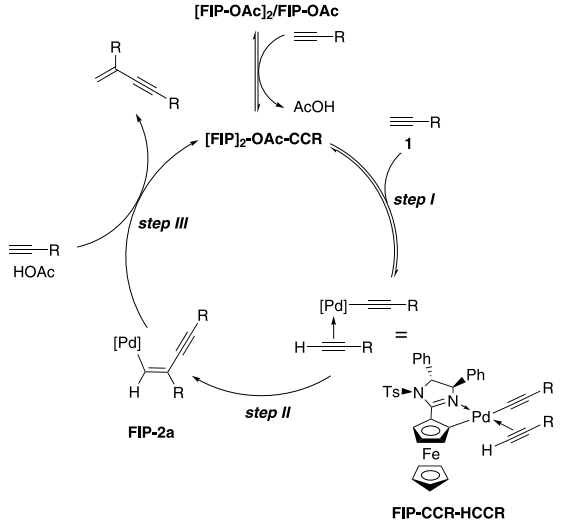

analogy to mechanism 2b)[13] in Scheme 1. Like in the mechanism for the stereo- and regioselective formation of (*E*)-**2** discussed above, the mechanism starts by formation of intermediate [FIP]$_2$-OAc-CCR. A subsequent acetylene coordination could give monometallic complex FIP-CCR-HCCR, in accordance to the observed regioselectivity. The steric demand of the ferrocene ligand is expected to be a key reason to cause R in the acetylene to point away from the ferrocene moiety in order to minimize repulsion.

To probe this interpretation of a monometallic mechanism, deuteration experiments were also performed in this case (Scheme 9). In the first experiment, nondeuterated acetylene was used in the presence of an excess of D_2O.

In agreement with mechanism 2b, in product **3** the position of H_B cis to the acetylene moiety is significantly more deuterated than H_A in trans position. A syn-palladation is thus dominating, as expected for a concerted insertion mechanism.[37]

Scheme 9. Deuteration Experiments under Conditions Favoring the Formation of 3 Using Different Sources

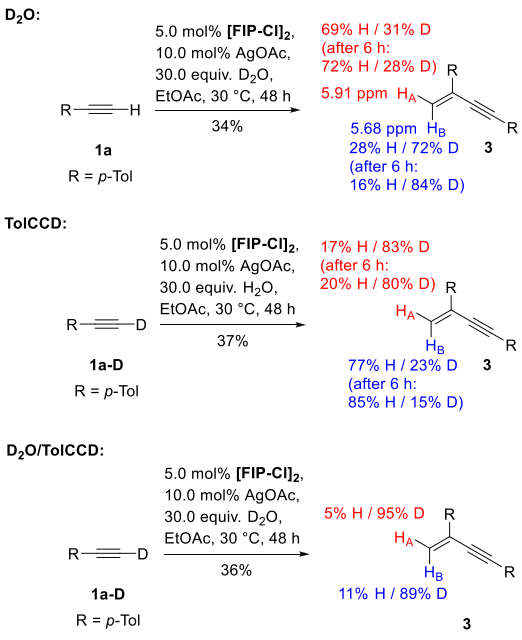

In the second experiment, deuterated acetylene substrate **1a-D** was utilized in the presence of an excess of H_2O. As expected, now position H_A in **3** is significantly more deuterated than H_B. The fact that the unexpected geometrical isomers are also formed in significant quantities in both experiments may be explained by H/D exchange of the alkyne via Pd−acetylide formation/protonolysis and time-dependent H scrambling, in agreement with the literature.[6a]

In the third experiment, deuterated acetylene substrate **1a-D** was utilized in the presence of excess D_2O. As expected, both terminal olefins positions were deuterated in product **3**.

Again VTNA was used to determine the empirical rate law.[34] The reaction reported in Table 4, entry 3, using **1c** as substrate, was monitored in EtOAc-d_8 at 30 °C for 14 h by ^{19}F NMR employing different concentrations of catalyst, **1c**, and water (for details, see Supporting Information). The following empirical rate law was determined:

$$r = k_{obs}[\text{catalyst}]^{0.4}[\mathbf{1c}]^{2.0}[H_2O]^{0.0}$$

The approximately half-order kinetic dependence in catalyst supports a monometallic active catalyst species formed from the bimetallic catalyst [FIP-OAc]$_2$. Again the rate law might be explained by a rate-determining C−C bond formation.

The fact that different mechanisms are involved depending on the solvent medium (product (*E*)-**2a** in MeCN via a bimetallic mechanism and product **3** in EtOAc via a monometallic mechanism) might be roughly explained by the stability of [FIP-CCR]$_2$, the key catalytic intermediate for the suggested bimetallic pathway. As shown above, it was found to be relatively stable in MeCN but not in EtOAc.

CONCLUSION

In summary, we have reported a regiodivergent dimerization of alkynes to form enynes employing a *C,N*-palladacycle catalyst. In contrast to previous studies using bimetallic catalysts, (*E*)-configured enynes were stereoselectively formed, very likely proceeding via a bis-palladium complex. A novel type of acetylide bis-Pd bridging was found in putative catalytic intermediates. Our studies suggest that a double $\mu-\kappa:\eta^2$ acetylide bridging enables a novel cooperative bimetallic syn-carbometalation pathway. However, depending on the reaction conditions, it is also possible to form the geminal regioisomer as major product utilizing the same catalyst. This might be related to the stability of the bis-Pd−bis-acetylide intermediate [FIP-CCR]$_2$ in MeCN which could be essential for the suggested bimetallic pathway. This intermediate was found to be unstable in other solvents including EtOAc, where formation of free ferrocene ligand and Pd black was noticed.[38]

ASSOCIATED CONTENT

Supporting Information

The Supporting Information is available free of charge at https://pubs.acs.org/doi/10.1021/acscatal.1c00473.

Experimental details, spectral data, and copies of ^1H and ^{13}C NMR spectra of all new compounds (PDF)

CIF files for [FIP]$_2$-OAc-CCR (R = *p*-$O_2N-C_6H_4$) (CIF)

https://doi.org/10.1021/acscatal.1c00473
ACS Catal. 2021, 11, 5496−5505

AUTHOR INFORMATION

Corresponding Author

René Peters − *Institut für Organische Chemie, Universität Stuttgart, D-70569 Stuttgart, Germany;* orcid.org/0000-0002-6668-4017; Email: rene.peters@oc.uni-stuttgart.de

Authors

Camilla Pfeffer − *Institut für Organische Chemie, Universität Stuttgart, D-70569 Stuttgart, Germany*

Nick Wannenmacher − *Institut für Organische Chemie, Universität Stuttgart, D-70569 Stuttgart, Germany*

Wolfgang Frey − *Institut für Organische Chemie, Universität Stuttgart, D-70569 Stuttgart, Germany*

Complete contact information is available at: https://pubs.acs.org/10.1021/acscatal.1c00473

Author Contributions

The manuscript was written through contributions of all authors. All authors have given approval to the final version of the manuscript.

Notes

The authors declare no competing financial interest.

ACKNOWLEDGMENTS

We thank Prof. Dr. Johannes Kästner and M. Sc. Juliane Heitkämper (both from University of Stuttgart, Institute for Theoretical Chemistry) as well as M. Sc. Konstantin Dorst and Dr. Carmen Schrapel (both from University of Stuttgart, Institute for Organic Chemistry) for helpful discussions.

REFERENCES

(1) (a) Mömming, M.; Kehr, G.; Wibbeling, B.; Fröhlich, R.; Schirmer, B.; Grimme, S.; Erker, G. Formation of Cyclic Allenes and Cumulenes by Cooperative Addition of Frustrated Lewis Pairs to Conjugated Enynes and Diynes. *Angew. Chem., Int. Ed.* **2010**, *49*, 2414−2417. (b) Arai, S.; Koike, Y.; Hada, H.; Nishida, A. Catalytic Dicyanative [4 + 2] Cycloaddition Triggered by Cyanopalladation of Conjugated Enynes under Aerobic Conditions. *J. Am. Chem. Soc.* **2010**, *132*, 4522−4523. (c) Nishimura, A.; Ohashi, M.; Ogoshi, S. Nickel-Catalyzed Intermolecular [2 + 2] Cycloaddition of Conjugated Enynes with Alkenes. *J. Am. Chem. Soc.* **2012**, *134*, 15692−15695. (d) Röse, P.; Garcia, C. C. M.; Pünner, F.; Harms, K.; Hilt, G. Cobalt-Catalyzed Cross-Benzannulation of Conjugated Enynes and Diynes. *J. Org. Chem.* **2015**, *80*, 7311−7316.

(2) Selected examples: (a) Dörfler, M.; Tschammer, N.; Hamperl, K.; Hübner, H.; Gmeiner, P. Novel D3 Selective Dopaminergics Incorporating Enyne Units as Nonaromatic Catechol Bioisosteres: Synthesis, Bioactivity, and Mutagenesis Studies. *J. Med. Chem.* **2008**, *51*, 6829−6838. (b) Hübner, H.; Haubmann, C.; Utz, W.; Gmeiner, P. Conjugated Enynes as Nonaromatic Catechol Bioisosteres: Synthesis, Binding Experiments, and Computational Studies of Novel Dopamine Receptor Agonists Recognizing Preferentially the D_3 Subtype. *J. Med. Chem.* **2000**, *43*, 756−762. (c) Jones, T. H.; Adams, R. M. M.; Spande, T. F.; Garraffo, H. M.; Kaneko, T.; Schultz, T. R. Histrionicotoxin Alkaloids Finally Detected in an Ant. *J. Nat. Prod.* **2012**, *75*, 1930−1936. (d) Nicolaou, K. C.; Dai, W. M.; Tsay, S. C.; Estevez, V. A.; Wrasidlo, W. Designed Enediynes: A New Class of DNA-Cleaving Molecules with Potent and Selective Anticancer Activity. *Science* **1992**, *256*, 1172−1178.

(3) Trost, B. M.; Sorum, M. T.; Chan, C.; Rühter, G. Palladium-Catalyzed Additions of Terminal Alkynes to Acceptor Alkynes. *J. Am. Chem. Soc.* **1997**, *119*, 698−708.

(4) Rivada-Wheelaghan, O.; Chakraborty, S.; Shimon, L. J. W.; Ben-David, Y.; Milstein, D. Z-Selective (Cross-)Dimerization of Terminal Alkynes Catalyzed by an Iron Complex. *Angew. Chem., Int. Ed.* **2016**, *55*, 6942−6945.

(5) Midya, G. C.; Paladhi, S.; Dhara, K.; Dash, J. Iron catalyzed highly regioselective dimerization of terminal aryl alkynes. *Chem. Commun.* **2011**, *47*, 6698−6700.

(6) Recent studies: (a) Liang, Q.; Osten, K. M.; Song, D. Iron-Catalyzed *gem*-Specific Dimerization of Terminal Alkynes. *Angew. Chem., Int. Ed.* **2017**, *56*, 6317−6320. (b) Liang, Q.; Hayashi, K.; Song, D. Catalytic Alkyne Dimerization without Noble Metals. *ACS Catal.* **2020**, *10*, 4895−4905. For a review see: (c) Xue, F.; Song, X.; Lin, T. T.; Munkerup, K.; Albawardi, S. F.; Huang, K.-W.; Hor, T. S. A.; Zhao, J. Dimerization of Terminal Aryl Alkynes Catalyzed by Iron(II) Amine-Pyrazolyl Tripodal Complexes with E/Z Selectivity Controlled by tert-Butoxide. *ACS Omega* **2018**, *3*, 5071−5077. (d) Gorgas, N.; Alves, L. G.; Stöger, B.; Martins, A. M.; Veiros, L. F.; Kirchner, K. Stable, Yet Highly Reactive Nonclassical Iron(II) Polyhydride Pincer Complexes: Z-Selective Dimerization and Hydroboration of Terminal Alkynes. *J. Am. Chem. Soc.* **2017**, *139*, 8130−8133. (e) Gorgas, N.; Stöger, B.; Veiros, L. F.; Kirchner, K. Iron(II) Bis(acetylide) Complexes as Key Intermediates in the Catalytic Hydrofunctionalization of Terminal Alkynes. *ACS Catal.* **2018**, *8*, 7973−7982. (f) Bhunia, M.; Sahoo, S. R.; Vijaykumar, G.; Adhikari, D.; Mandal, S. K. Cyclic (Alkyl)amino Carbene Based Iron Catalyst for Regioselective Dimerization of Terminal Arylalkynes. *Organometallics* **2016**, *35*, 3775−3780. (g) Liang, Q.; Sheng, K.; Salmon, A.; Zhou, V. Y.; Song, D. Active Iron(II) Catalysts toward gem-Specific Dimerization of Terminal Alkynes. *ACS Catal.* **2019**, *9*, 810−818.

(7) (a) Bassetti, M.; Pasquini, C.; Raneri, A.; Rosato, D. Selective Dimerization of Arylalkynes to (*E*)-1,4-Diaryl Enynes Catalyzed by the $[Ru(p\text{-cymene})Cl_2]_2$/Acetic Acid System under Phosphine-Free Conditions. *J. Org. Chem.* **2007**, *72*, 4558−4561. (b) Yi, C. S.; Liu, N. Homogeneous Catalytic Dimerization of Terminal Alkynes by $C_5Me_5Ru(L)H_3$ (L = PPh_3, PCy_3, PMe_3). *Organometallics* **1996**, *15*, 3968−3971. (c) Yi, C. S.; Liu, N. The Ruthenium Acetylide Catalyzed Cross-Coupling Reaction of Terminal and Internal Alkynes: Isolation of a Catalytically Active *β*-Agostic Intermediate Species. *Organometallics* **1998**, *17*, 3158−3160.

(8) (a) Chen, J.-F.; Li, C. Cobalt-Catalyzed gem-Cross-Dimerization of Terminal Alkynes. *ACS Catal.* **2020**, *10*, 3881−3889. (b) Grenier-Petel, J.-C.; Collins, S. K. Photochemical Cobalt-Catalyzed Hydroalkynylation to Form 1,3-Enynes. *ACS Catal.* **2019**, *9*, 3213−3218. (c) Xu, D.; Sun, Q.; Quan, Z.; Wang, C.; Sun, W. Cobalt-Catalyzed Dimerization and Homocoupling of Terminal Alkynes. *Asian J. Org. Chem.* **2018**, *7*, 155−159. (d) Zhuang, X.; Chen, J.-Y.; Yang, Z.; Jia, M.; Wu, C.; Liao, R.-Z.; Tung, C.-H.; Wang, W. Sequential Transformation of Terminal Alkynes to 1,3-Dienes by a Cooperative Cobalt Pyridonate Catalyst. *Organometallics* **2019**, *38*, 3752−3759.

(9) Lee, C.-C.; Lin, Y.-C.; Liu, Y.-H.; Wang, Y. Rhodium-Catalyzed Dimerization of Terminal Alkynes Assisted by MeI. *Organometallics* **2005**, *24*, 136−143.

(10) Ghosh, R.; Zhang, X.; Achord, P.; Emge, T. J.; Krogh-Jespersen, K.; Goldman, A. S. Dimerization of Alkynes Promoted by a Pincer-Ligated Iridium Complex. C−C Reductive Elimination Inhibited by Steric Crowding. *J. Am. Chem. Soc.* **2007**, *129*, 853−866.

(11) Rubina, M.; Gevorgyan, V. Can Agostic Interaction Affect Regiochemistry of Carbopalladation? Reverse Regioselectivity in the Palladium-Catalyzed Dimerization of Aryl Acetylenes. *J. Am. Chem. Soc.* **2001**, *123*, 11107−11108.

(12) Yang, C.; Nolan, S. P. Regio- and Stereoselective Dimerization of Terminal Alkynes to Enynes Catalyzed by a Palladium/Imidazolium System. *J. Org. Chem.* **2002**, *67*, 591−593.

(13) Zatolochnaya, O. V.; Gordeev, E. G.; Jahier, C.; Ananikov, V. P.; Gevorgyan, V. Carboxylate Switch between Hydro- and Carbopalladation Pathways in Regiodivergent Dimerization of Alkynes. *Chem. - Eur. J.* **2014**, *20*, 9578−9588.

(14) Jahier, C.; Zatolochnaya, O. V.; Zvyagintsev, N. V.; Ananikov, V. P.; Gevorgyan, V. General and Selective Head-to-Head Dimerization of Terminal Alkynes Proceeding via Hydropalladation Pathway. *Org. Lett.* **2012**, *14*, 2846−2849.

(15) Islas, R. E.; Cárdenas, J.; Gaviño, R.; García-Ríos, E.; Lomas-Romero, L.; Morales-Serna, J. A. Phosphinito palladium(II) complexes as catalysts for the synthesis of 1,3-enynes, aromatic alkynes and ynones. *RSC Adv.* **2017**, *7*, 9780−9789.
(16) Sun, S.; Kroll, J.; Luo, Y.; Zhang, L. Gold-Catalyzed Regioselective Dimerization of Aliphatic Terminal Alkynes. *Synlett* **2012**, *2012*, 54−56.
(17) Duchateau, R.; van Wee, C. T.; Teuben, J. H. Insertion and C-H Bond Activation of Unsaturated Substrates by Bis(benzamidinato) yttrium Alkyl, $[PhC(NSiMe_3)_2]_2YR$ (R = CH_2Ph·THF, $CH(SiMe_3)_2$), and Hydrido, $\{[PhC(NSiMe_3)_2]_2Y(\mu\text{-}H)\}_2$, Compounds. *Organometallics* **1996**, *15*, 2291−2302.
(18) (a) Al: Korolev, A. V.; Guzei, I. A.; Jordan, R. F. Reactivity of Cationic Organoaluminum Aminotroponiminate Compounds with Unsaturated Substrates. Formation of Dinuclear Dicationic Aluminum Complexes. *J. Am. Chem. Soc.* **1999**, *121*, 11605−11606. (b) B: Hasenbeck, M.; Müller, T.; Gellrich, U. Metal-free gem Selective Dimerization of Terminal Alkynes Catalyzed by a Pyridonate Borane Complex. *Catal. Sci. Technol.* **2019**, *9*, 2438−2444. (c) KOtBu: Ahmed, J.; Swain, A. K.; Das, A.; Govindarajan, R.; Bhunia, M.; Mandal, S. K. A K-Arylacetylide Complex for Catalytic Terminal Alkyne Functionalization Using KOtBu as a Precatalyst. *Chem. Commun.* **2019**, *55*, 13860−13863.
(19) (a) Buxaderas, E.; Alonso, D. A.; Nájera, C. Microwave-assisted palladium-catalyzed highly regio- and stereoselective head to head dimerization of terminal aryl alkynes in water. *RSC Adv.* **2014**, *4*, 46508−46512. (b) Midya, G. C.; Paladhi, S.; Dhara, K.; Dash, J. Iron catalyzed highly regioselective dimerization of terminal aryl alkynes. *Chem. Commun.* **2011**, *47*, 6698−6700. (c) Kiyota, S.; Soeta, H.; Komine, N.; Komiya, S.; Hirano, M. *E*-Selective dimerization of phenylacetylene catalyzed by cationic tris(μ-hydroxo)diruthenium(II) complex and the mechanistic insight: The role of two ruthenium centers in catalysis. *J. Mol. Catal. A: Chem.* **2017**, *426*, 419−428.
(20) Nishiura, M.; Hou, Z.; Wakatsuki, Y.; Yamaki, T.; Miyamoto, T. Novel Z-Selective Head-to-Head Dimerization of Terminal Alkynes Catalyzed by Lanthanide Half-Metallocene Complexes. *J. Am. Chem. Soc.* **2003**, *125*, 1184−1185.
(21) Bassetti, M.; Pasquini, C.; Raneri, A.; Rosato, D. Selective Dimerization of Arylalkynes to (*E*)-1,4-Diaryl Enynes Catalyzed by the $[Ru(p\text{-cymene})Cl_2]_2$/Acetic Acid System under Phosphine-Free Conditions. *J. Org. Chem.* **2007**, *72*, 4558−4561.
(22) Qü, J.-P.; Masui, D.; Ishii, Y.; Hidai, M. Head-to-head Z Dimerization of Terminal Alkynes Catalyzed by Thiolate-bridged Diruthenium Complexes. *Chem. Lett.* **1998**, *27*, 1003−1004.
(23) Chen, T.; Guo, C.; Goto, M.; Han, L.-B. A Brønsted acid-catalyzed generation of palladium complexes: efficient head-to-tail dimerization of alkynes. *Chem. Commun.* **2013**, *49*, 7498−7500.
(24) Gao, Y.; Puddephatt, R. J. Selective head-to-tail dimerization of phenylacetylene catalyzed by a diruthenium μ-methylene complex. *Inorg. Chim. Acta* **2003**, *350*, 101−106.
(25) Trost, B. M.; Chan, C.; Ruhter, G. Metal-Mediated Approach to Enynes. *J. Am. Chem. Soc.* **1987**, *109*, 3486−3487.
(26) Later, a chloride bridged dimeric Pd(II) complex was reported providing geminal product **3**, again showing that the steric bulk within the ligand system favors the formation of this regioisomer: Islas, R. E.; Cárdenas, J.; Gaviño, R.; García-Ríos, E.; Lomas-Romero, L.; Morales-Serna, J. A. Phosphinito palladium(II) complexes as catalysts for the synthesis of 1,3-enynes, aromatic alkynes and ynones. *RSC Adv.* **2017**, *7*, 9780−9789.
(27) Lauer, M. G.; Headford, B. R.; Gobble, O. M.; Weyhaupt, M. B.; Gerlach, D. L.; Zeller, M.; Shaughnessy, K. H. A Trialkylphosphine-Derived Palladacycle as a Catalyst in the Selective Cross-Dimerization of Terminal Arylacetylenes with Terminal Propargyl Alcohols and Amides. *ACS Catal.* **2016**, *6*, 5834−5842.
(28) Reviews on bimetallic catalysis with late transition metals: (a) van den Beuken, E. K.; Feringa, B. L. Bimetallic catalysis by late transition metal complexes. *Tetrahedron* **1998**, *54*, 12985−13011. (b) Weiss, M.; Peters, R. Bimetallic Catalysis: Cooperation of Carbophilic Metal Centers In *Cooperative Catalysis − Designing Efficient Catalysts for Synthesis*; Peters, R., Ed.; Wiley-VCH: Weinheim, 2015.
(29) For a mixed Pd/Pt system, see: Fornies, J.; Gomez-Saso, M. A.; Lalinde, E.; Martinez, F.; Moreno, M. T. Preparation of Doubly Acetylide-Bidged Binuclear Platinum-Platinum and Platinum-Palladium Complexes. Structures of $[[(dppe)Pt(CCPh)_2]Pt(C_6F_5)_2]$ and $(PMePh_3)_2[(C_6F_5)_2Pt(\mu\text{-}CCPh)_2Pt(C_6F_5)_2]$. *Organometallics* **1992**, *11*, 2873−2883.
(30) FIP: (a) Weiss, M. E.; Fischer, D. F.; Xin, Z.-q.; Jautze, S.; Schweizer, W. B.; Peters, R. Practical, Highly Active, and Enantioselective Ferrocenyl−Imidazoline Palladacycle Catalysts (FIPs) for the Aza-Claisen Rearrangement of N-para-Methoxyphenyl Trifluoroacetimidates. *Angew. Chem., Int. Ed.* **2006**, *45*, 5694−5699. (b) Xin, Z.-q.; Fischer, D. F.; Peters, R. Catalytic Asymmetric Formation of Secondary Allylic Amines by Aza-Claisen Rearrangement of Trifluoroacetimidates. *Synlett* **2008**, *2008*, 1495−1499. (c) Peters, R.; Xin, Z.-q.; Maier, F. Catalyst versus Substrate Induced Selectivity: Kinetic Resolution by Palladacycle Catalyzed Allylic Imidate Rearrangements. *Chem. - Asian J.* **2010**, *5*, 1770−1774. (d) Peters, R.; Fischer, D. F.; Jautze, S. Ferrocene and Half Sandwich Complexes as Catalysts with Iron Participation. *Top. Organomet. Chem.* **2011**, *33*, 139−175. (e) Hellmuth, T.; Frey, W.; Peters, R. Regioselective Catalytic Asymmetric C-Alkylation of Isoxazolinones by a Base-Free Palladacycle-Catalyzed Direct 1,4-Addition. *Angew. Chem., Int. Ed.* **2015**, *54*, 2788−2791. (f) Schrapel, C.; Peters, R. Exogenous-Base-Free Palladacycle-Catalyzed Highly Enantioselective Arylation of Imines with Arylboroxines. *Angew. Chem., Int. Ed.* **2015**, *54*, 10289−10293. (g) Peters, R.; Fischer, D. F.; Jautze, S. Ferrocene and Half Sandwich Complexes as Catalysts with Iron Participation. *Top. Organomet. Chem.* **2011**, *33*, 139−175. (h) Schrapel, C.; Frey, W.; Garnier, D.; Peters, R. Highly Enantioselective Ferrocenyl Palladacycle-Acetate Catalysed Arylation of Aldimines and Ketimines with Arylboroxines. *Chem. - Eur. J.* **2017**, *23*, 2448−2460. (i) Li, J.; Yu, B.; Lu, Z. Chiral Imidazoline Ligands and Their Applications in Metal-Catalyzed Asymmetric Synthesis. *Chin. J. Chem.* **2021**, *39*, 488−514.
(31) FBIP: (a) Jautze, S.; Seiler, P.; Peters, R. Macrocyclic Ferrocenyl Bisimidazoline Palladacycle Dimers (FBIPs) as Highly Active and Enantioselective Catalysts for the Aza-Claisen Rearrangement of (Z)-Configured N-para-Methoxyphenyl Trifluoroacetimidates. *Angew. Chem., Int. Ed.* **2007**, *46*, 1260−1264. (b) Jautze, S.; Peters, R. Bimetallic Enantioselective Catalysis of Michael Additions Forming Quaternary Stereocenters. *Angew. Chem., Int. Ed.* **2008**, *47*, 9284−9288. (c) Jautze, S.; Diethelm, S.; Frey, W.; Peters, R. Diastereoselective Bis-Cyclopalladation of Ferrocene-1,1′-diyl Bis-Imidazolines: Translation of Central via Axial into Planar Chirality. *Organometallics* **2009**, *28*, 2001−2004. (d) Weber, M.; Jautze, S.; Frey, W.; Peters, R. Bispalladacycle-Catalyzed Brønsted Acid/Base-Promoted Asymmetric Tandem Azlactone Formation−Michael Addition. *J. Am. Chem. Soc.* **2010**, *132*, 12222−12225. (e) Weiss, M.; Peters, R. Catalytic Direct Dehydrogenative Cross-Couplings of C−H (Pro)Nucleophiles and Allylic Alcohols without an Additional Oxidant. *ACS Catal.* **2015**, *5*, 310−316. (f) Weber, M.; Klein, J. E. M. N.; Miehlich, B.; Frey, W.; Peters, R. Monomeric Ferrocene Bis-Imidazoline Bis-Palladacycles: Variation of Pd−Pd Distances by an Interplay of Metallophilic, Dispersive, and Coulombic Interactions. *Organometallics* **2013**, *32*, 5810−5817. (g) Weiss, M.; Peters, R. Catalytic Direct Dehydrogenative Cross-Couplings of C−H (Pro)-Nucleophiles and Allylic Alcohols without an Additional Oxidant. *ACS Catal.* **2015**, *5*, 310−316. (h) Yu, X.; Wannenmacher, N.; Peters, R. Stereospecific Asymmetric Synthesis of Tertiary Allylic Alcohol Derivatives by Catalytic [2,3]-Meisenheimer Rearrangements. *Angew. Chem., Int. Ed.* **2020**, *59*, 10944−10948.
(32) There is one example in the literature providing 65% of the major isomer: Iona, R.; Bassetti, M. Dimerization of Aromatic Terminal Alkynes Featuring Hydrophilic Functional Groups under Ruthenium and Acid Promoted Catalysis. Competitive Alkyne Hydration upon Substituent Effect. *ChemistrySelect* **2020**, *5* (22), 6666−6669.

https://doi.org/10.1021/acscatal.1c00473
ACS Catal. 2021, 11, 5496−5505

(33) Blackmond, D. G. Reaction Progress Kinetic Analysis: A Powerful Methodology for Mechanistic Studies of Complex Catalytic Reactions. *Angew. Chem., Int. Ed.* **2005**, *44*, 4302−4320.
(34) (a) Burés, J. A Simple Graphical Method to Determine the Order in Catalyst. *Angew. Chem., Int. Ed.* **2016**, *55*, 16084−16087. (b) Nielsen, C. D.-T.; Burés, J. Visual kinetic analysis. *Chem. Sci.* **2019**, *10*, 348−353.
(35) For Pt complexes with a related bridging mode, see: Berenguer, J. R.; Lalinde, E.; Moreno, M. T. An overview of the chemistry of homo and heteropolynuclear platinum complexes containing bridging acetylide (μ-C≡CR) ligands. *Coord. Chem. Rev.* **2010**, *254*, 832−875.
(36) Heating preformed $[FIP\text{-}CCR]_2$ under the conditions of Scheme 4 (i.e., in the absence of HOAc/NaOAc/H_2O) did not result in the smooth formation of **2**-$[Pd]_2$ and only decomposition was observed. The fact that **2**-$[Pd]_2$ is not readily formed is in agreement with a slow C−C bond formation.
(37) Steinborn, D. *Fundamentals of Organometallic Catalysis*; Wiley-VCH: Weinheim, 2012.
(38) As we see Glaser coupling as a side reaction, we think that this is one of the major reasons for catalyst decomposition.

https://doi.org/10.1021/acscatal.1c00473
ACS Catal. 2021, 11, 5496−5505